

Ari J. Tuononen and Lassi Hartikainen. 2008. Optical position detection sensor to measure tyre carcass deflections in aquaplaning. *International Journal of Vehicle Systems Modelling and Testing*, volume 3, number 3, pages 189-197.

© 2008 by authors and © 2008 Inderscience Enterprises

Preprinted with permission.

# Optical Position Detection Sensor to Measure Tyre Carcass Deflections in Aquaplaning

## Abstract

Information about the available friction of individual tyres is crucial for the operation of different ADAS systems, such as collision mitigation and ACC. The information about aquaplaning is especially useful because aquaplaning severely hampers tyre-road interaction. In addition, validation tools are needed for complex physical tyre models, which are common development and research tools in the tyre industry. The optical tyre sensor is capable of accurately measuring the deformations in the inner ring of the tyre. Partial and full aquaplaning can be detected using the sensor. It also provides a research tool for understanding the phenomenon itself.

Keywords: aquaplaning; hydroplaning; optical tyre sensor; tyre deformation; wet friction; friction; estimation; FEM; CFD

## Introduction

All the significant forces and moments acting on a vehicle, except for aerodynamic forces and gravity, are generated by the tyres. The aquaplaning of the tyre severely hampers this interaction, and consequently may lead to a situation where the vehicle cannot be controlled by driver inputs.

Estimation of friction potential is vital for many ADAS (Advanced Driver Assistance Systems) applications, such as collision mitigation systems and adaptive cruise control (ACC). Aquaplaning is a special case for friction-potential estimation. It is also one of the most important cases, because of the sudden impact and because it may mislead other estimators if not correctly recognised. For example, if a vehicle begins to yaw during aquaplaning, the ESC (Electronic Stability Control) system could choose the tyre that has full contact for brake intervention. The information about the tyres not having full road-contact could help the ABS (Anti-lock Braking System) as well. Furthermore, it is difficult to detect the early stages of aquaplaning with the existing wheel-speed sensors.

The concept of aquaplaning has been assessed with simplified physical models like the so-called *Gleitfilmmodell* (Essers, 1987), as well as with more complicated approaches that also model the tyre geometry and the water flow using tools like FEA (Finite Element Analysis) and CFD (Computational Fluid Dynamics). The tyre-road contact during aquaplaning has traditionally been divided into three zones (Browne, 1972). The zones are shown in Figure 1. In zone A, the inertial effect of the water dominates and no contact between the tyre and the road surface exists. In zone B, some rubber-road contact exists, but the viscous effect of the water squeezing out from the contact area limits this area. Zone C represents full wet road contact. A more recent study about wet road friction has been carried out by Persson (2004). The study relates especially to zone C in Figure 1.

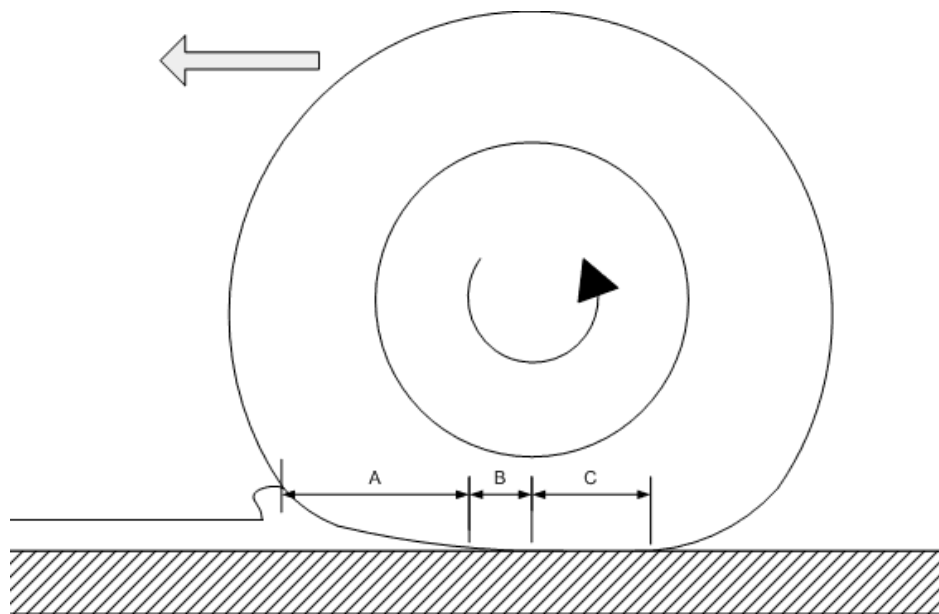


**Figure 1 Three-zone concept**

Road wetness has been evaluated from tyre noise in (Eichhorn, 1992). The sound pressure level on a wet surface increases for frequencies higher than 1 kHz. The same article also clarified how the tyre tread deformation sensor could be used to evaluate road characteristics.

Tread block deformations during aquaplaning have been measured with the Darmstadt tyre sensor (Stöcker, 1993). The points where the tread block came into contact with the water surface and then the road surface were detected. A simple algorithm using the local maxima of these points was presented to detect the early stages of aquaplaning. The algorithm, however, only applies when both peaks exist.

In addition to supporting the active safety systems, there is another field of application for the optical tyre sensor. Recently, the Finite Volume Method (FVM) and the Finite Element Method (FEM) have been implemented in studying tyre behaviour during full or early aquaplaning conditions by, for example, Nakajima (2000) and Cho (2006). However, not all the measurements that would be needed to validate such a model are widely available. The optical tyre sensor can measure tyre carcass displacement under dynamic driving conditions. The measurement results are needed to gain a qualitative understanding of the aquaplaning phenomenon and for a validation of complicated tyre models, which have become a common development tool for the tyre industry.

## **Methods**

The optical tyre sensor was developed in the EC-funded APOLLO-project 2002-2005 and was further developed in EC-project FRICTI@N. The operating principle of the sensor is explained in, for example, (APOLLO, 2005). The construction of the tyre is shown in Figures 2 and 3. The wireless data transmission operated at 5000 Hz and 12 bits

for four channels. Because the intensity of the LED is a function of angle, tilting the LED changes the intensity on the PSD sensor. This has to be taken into account when interpreting the results, particularly the intensity.

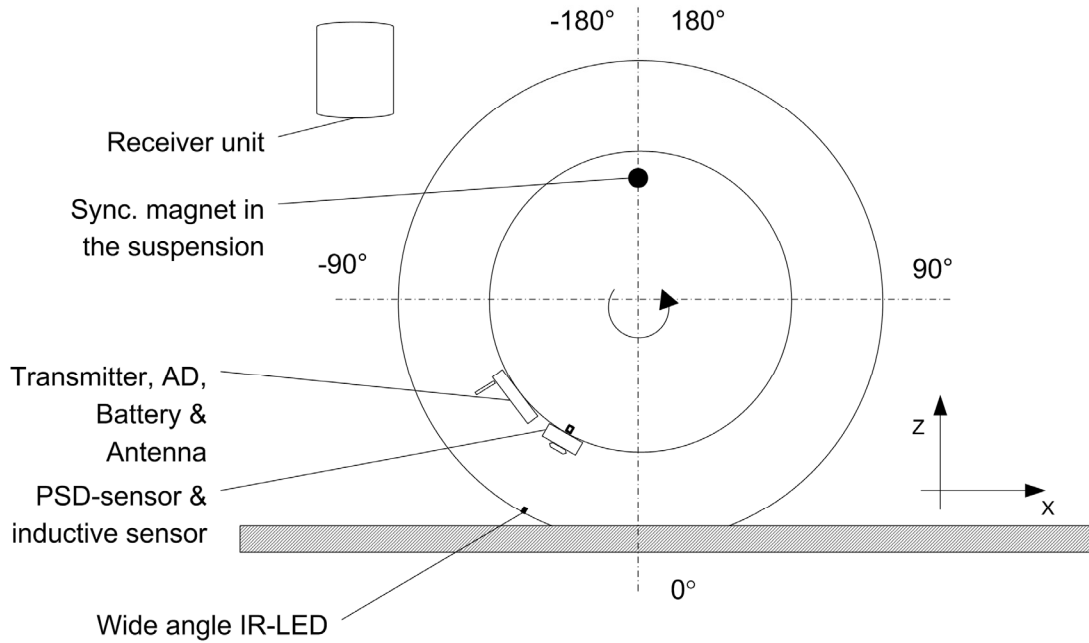


**Figure 2 Optical tyre sensor components**

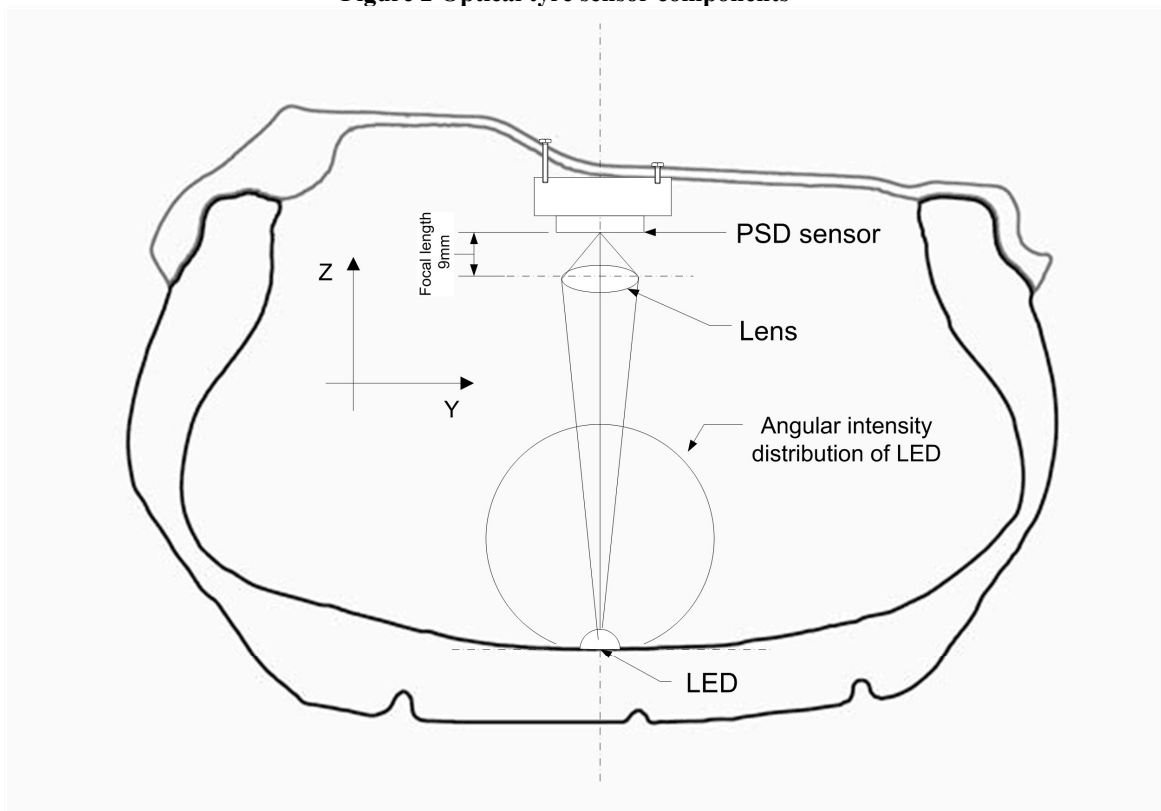


**Figure 3 Measurement principle of the optical tyre sensor**

A non-studded Nokian WR winter tyre was selected for the tests. The tyre size was 205/55/16 and tyre pressure 2.6 bar. The test vehicle was a VW Golf V Variant 1.9 TDI and the tyre sensor was positioned on the left front wheel (Figure 4). In addition to the optical sensor, a magnetic pick-up sensor was installed into the rim to synchronise tyre sensor data with the rotation angle. If the tyre sensor signal itself had been utilized to detect the contact, the phase shifts could not have been evaluated as reliably.



Figure 4 Measurement vehicle and tyre sensor (front left) with the radio receiver

The ambient temperature at the outside of the test track was 14°C. The track is sketched in Figure 5. The tarmac surface was dry before the water reservoir and wet after the reservoir. This article focuses on the dry tarmac and the water sections.

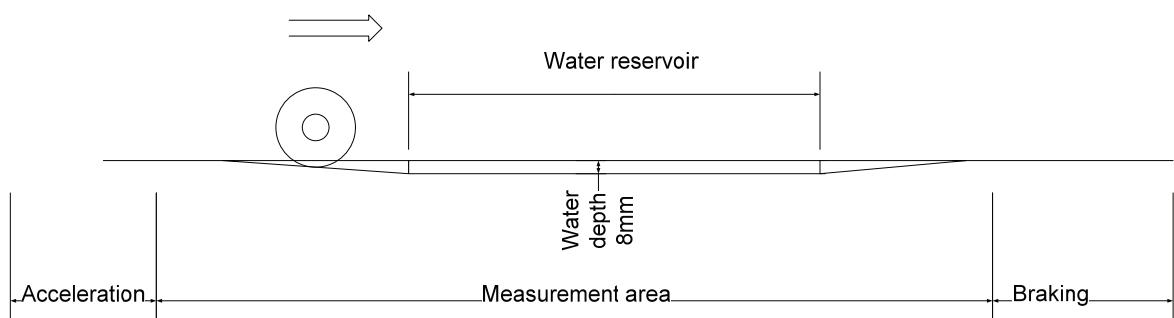


Figure 5 Aquaplaning proving ground

Data was gathered and later analysed with different driving manoeuvres. It was not clear beforehand whether the ESC system of the vehicle should be turned on or off for the measurements. Additionally, using the cruise control might sound ideal but, unfortunately, the system does not work if the traction wheels are without proper road contact. Therefore, just before entering the water, either clutch or throttle was fully depressed. Both actions were tried with the ESC on and off. Most runs were made at 110km/h, but a few runs at 90, 80 and 70 km/h were made as well. All the low-speed

measurements were made with the clutch fully depressed and the ESC turned off. The intention was not to compare aquaplaning behaviour with or without ESC, but to minimize the influence of rapid deceleration on the wheel in full aquaplaning.

The measurement procedure was the same for every run. The inflation pressure of the sensor tyre was measured before every other run and ESC was selected for the specific run. The data acquisition was started and the vehicle was accelerated to the desired velocity; this was kept constant.

Because the measurements were made inside a rotating tyre, the tyre sensor data is cyclic; therefore, plotting the data with time on the x-axis is not very illustrative. This is why the data was analysed by creating a rotation angle vector using the time vector and a pulse from the inductive sensor. When the inductive sensor signal crosses zero, the rotation angle is set to  $-180^\circ$ , which is the sensor-up position. The gap between the two sensor-up positions is defined as an angle vector. The angle vector consists of 600 points linearly spaced between  $-180^\circ$  and  $180^\circ$ . Then the original data is interpolated for this new angle vector and rotations can be compared independently.

In addition to detecting the rotation angle of the tyre, it was important to detect the water reservoir section reliably. Hence, a data trigger operated by the co-driver was installed into the instrument board of the test vehicle.

## **Results and analysis**

The average intensity (radial displacement) curves for one whole measurement run are shown in Figure 6. The acceleration on tarmac and the braking after the water dominate the values, especially near the area of contact, which is around a zero angle. Figure 7 shows the longitudinal movement of the LED during the same measurement run. The vertical transition of the curves shows how braking moves the tyre carcass in relation to the wheel and how acceleration moves it in the opposite direction.

In order to analyse the influence of the water layer on tyre carcass displacements, the acceleration and braking sections were removed from the analysed data. The two transition points were marked during the measurements with a data trigger. Three wheel rotations before and three after the first transition point were removed from the data. This was done to avoid the effects of the descending ramp when entering the water (Figure 5). Ten rotations before the removed ones, and the next ten after, were used for the actual analysis. The average curves and standard deviation of these rotations before and after entering the water are seen in Figure 8 and Figure 9.

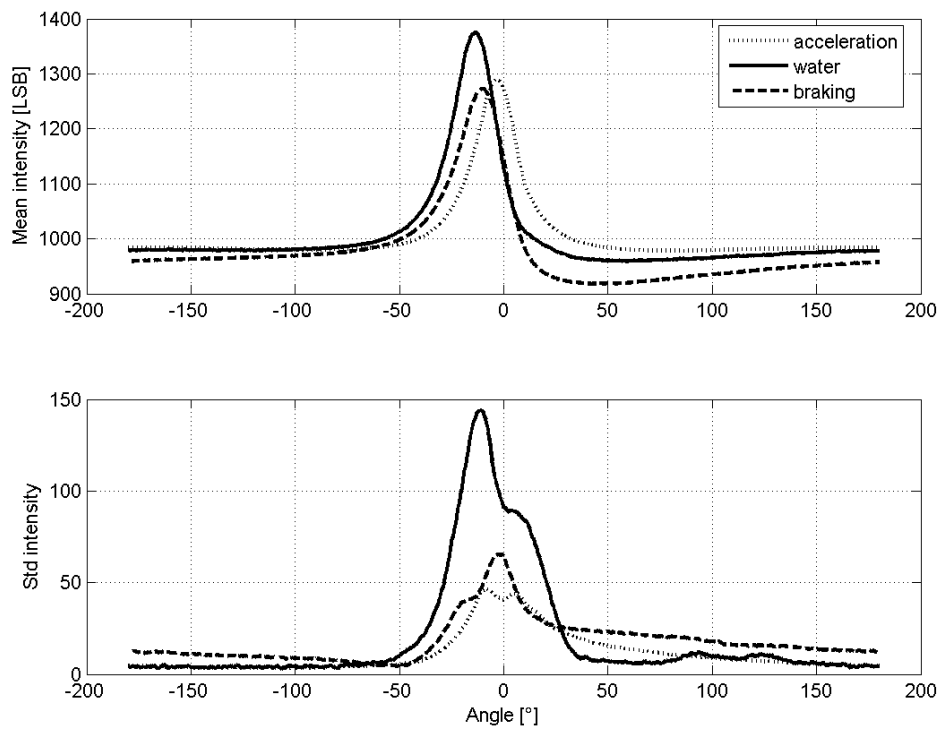


**Figure 6** The mean intensity and standard deviation curves for a complete measurement run

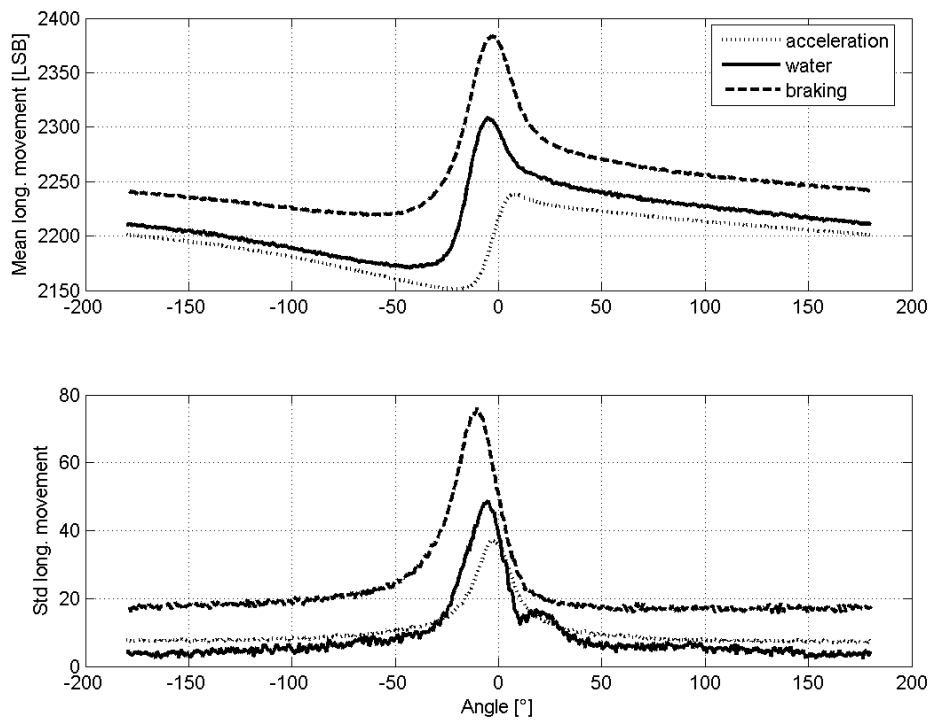


**Figure 7** The mean longitudinal and standard deviation curves for a complete measurement run

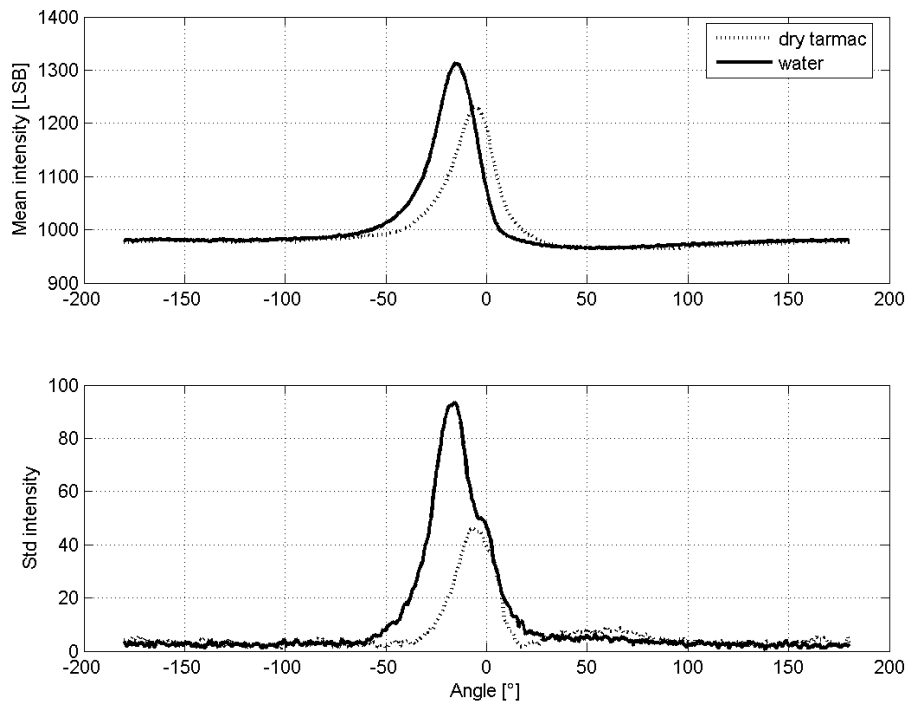


**Figure 8** The mean intensity and standard deviation before and after driving into the water at 110km/h

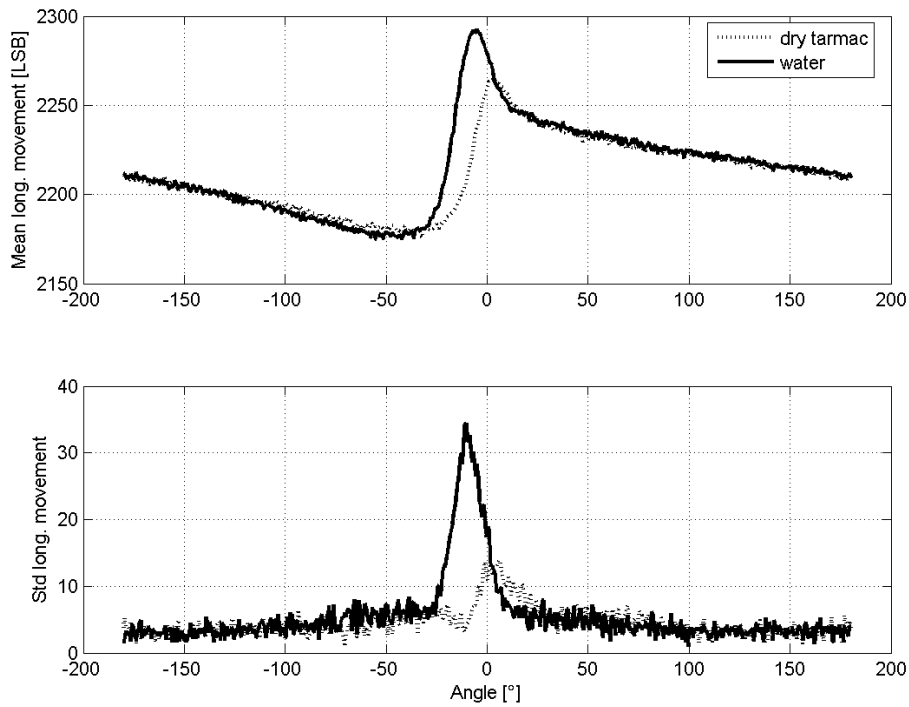


**Figure 9** The mean longitudinal movement and standard deviation before and after driving into the water at 110km/h

In the water, the peak values of both the radial movement of the LED, indicated by the intensity, as well as the longitudinal movement, are increased and shifted towards smaller rotation angles. This effect was observed also in measurement runs driven with full throttle. The standard deviation in both signals is significantly higher, due to the effect of the water and the slight change in the vehicle elevation when descending into the water. Furthermore, the standard deviation in water follows the dry tarmac curves after the centre of contact, which could indicate viscous zone (Figure 1, Zone B) to begin.

In order to illustrate the results in a more comprehensive way, the intensity data was converted to the polar coordinate system. The data was arbitrarily scaled, which means that the metric values shown in Figure 10 and Figure 11 are not accurate. They should, however, be of the right order. In the figures, the tyre is rolling to the left. The purpose of the horizontal dash-dot line and the perfect circle is to illustrate the differences between the curves. A clear difference exists between the first one driven at 110 km/h and the second one at 80 km/h.

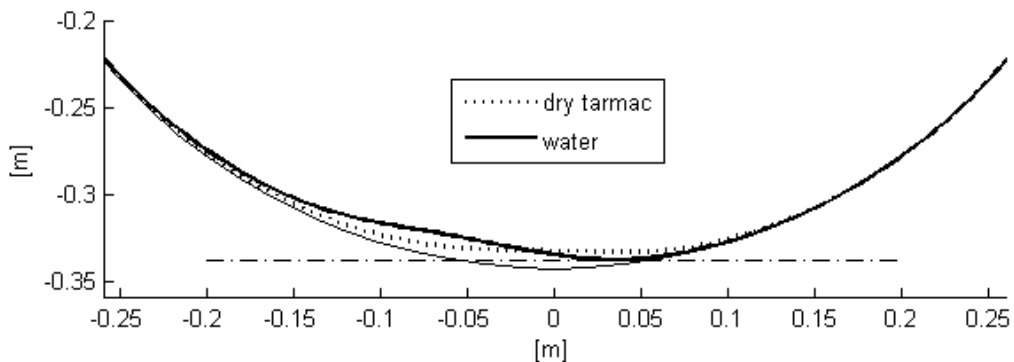


**Figure 10 Tyre inner ring deformation during full aquaplaning at 110 km/h**

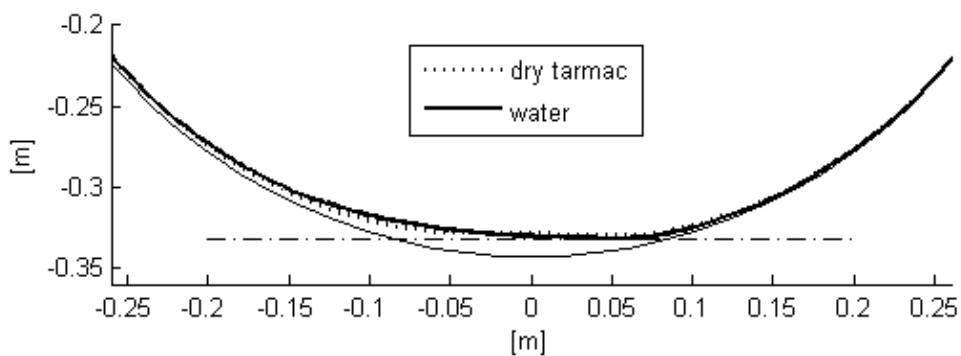


**Figure 11 Tyre inner ring deformation during partial aquaplaning at 80 km/h**

The results shown in Figures 6 and 8 are in good agreement with the tread block deformation data presented in (Stöcker, 1993). The measured quantities are different in these sensors, but the sensor outputs can be compared in a qualitative sense and same phenomenon can be observed in both. The radial deformation of the tread block, when coming into the contact patch, seems to shift towards smaller tyre rotation angles. In the optical tyre sensor data, this movement is filtered by the tyre belt, but yet is clearly

visible (Figure 8). The radial deformation of the tyre inner ring starts earlier due to the inertial effect of the water.

## **Discussion**

When driving on dry tarmac, the contact pressure between the tyre and the road acts on the tips of the tread blocks causing the tread blocks to deform. If there is a significant water film on the road, or if the tyre is rolling on a soft surface, part of the contact pressure acts on the tyre surface between the tread blocks, causing less tread block deformation. Because the optical tyre sensor measures the distance between the wheel and the tyre inner ring rather than the ground, the change in tread deformation affects the results.

The optical tyre sensor seems to offer a measurement tool for assessing the aquaplaning phenomenon from a direct point of view. This helps us understand tyre behaviour under complex conditions. The technique would be especially useful in validating results from tyre-model simulations, such as FEM.

Tyre sensors have the potential of becoming part of a vehicle in visionary accident-free traffic. However, before the sensor can be commercialised, many generations of research-type sensors are needed in order to develop the necessary algorithms and to advance the study of tyre behaviour in general.

Further research will focus on real-time estimation of aquaplaning, taking into account the degree of aquaplaning also. In addition, the calibration procedures will be enhanced in order to reliably obtain displacements of the tyre carcass in metric scale.

## **Acknowledgements**

This work was financially supported by EU-project FRICTION FP6-IST-2004-4-027006. This support is gratefully acknowledged.

## **References**

APOLLO project, Final report (2005) Available online at: [www.vtt.fi/apollo](http://www.vtt.fi/apollo)

Cho J.R., Choi J.H., Lee H.W., Woo J.S. (2007) Braking Distance Prediction by Hydroplaning Analysis of 3-D Patterned Tire Model. *Journal of System Design and Dynamics*, Vol.1, No. 3, 2007.

Cho J.R., Lee H.W., Sohn J.S., Kim G.J., Woo J.S (2006) Numerical investigation of hydroplaning characteristics of three-dimensional patterned tire. *European Journal of Mechanics - A/Solids* Vol. 25, Issue 6.

Eichhorn, U., Roth, J. (1992) Prediction and Monitoring of Tyre/Road friction. In FISITA 24th Congress: Safety, the Vehicle and the Road: Technical Papers Vol. 2.

Essers,U., Haken,K.A., Wolf, A. (1987) Einfluss der Strassenoberfläche auf Fahrsicherheit bei Nässe, VDI Berichte 650.

Seta, E., Nakajima, Y., Kamegawa, T., Ogawa, H. (2000) Hydroplaning Analysis by FEM and FVM: Effect of Tire Rolling and Tire Pattern on Hydroplaning. Seoul 2000 FISITA World Automotive Congress, June 12-15. Seoul, Korea.

Persson, BNJ., Tartaglino, U., Albohr, O., Tosatti, E. (2004) Sealing is at the origin of rubber slipping on wet roads. Nature materials, Vol. 3, p. 882-885.

Stöcker, J. et al. (1993) Erkennung inhomogener Kraftschlußverhältnisse zwischen Reifen und Fahrbahn am Beispiel Aquaplaning, VDI Berichte 1088.